DOI: https://doi.org/10.1016/j.heares.2022.108679

Scaling of ear morphology across 127 bird species and its implications for hearing performance

Jeffrey N. Zeyl[a*], Edward P. Snelling[b], Rocío Joo[c,d], Susana Clusella-Trullas[a]

[a] Department of Botany and Zoology, Stellenbosch University, Stellenbosch, South Africa

[b] Department of Anatomy and Physiology, and Centre for Veterinary Wildlife Research, Faculty of Veterinary Science, University of Pretoria, Onderstepoort, South Africa

[c] Department of Wildlife Ecology and Conservation, Fort Lauderdale Research and Education Center, University of Florida, Davie, FL, USA

[d] Global Fishing Watch, Washington, DC 20036, USA

* Author for correspondence (jeffzeyl@gmail.com),

Abstract

The dimensions of auditory structures among animals of varying body size can have implications for hearing performance. Larger animals often have a hearing range focused on lower frequencies than smaller animals, which may be explained by several anatomical mechanisms in the ear and their scaling relationships. While the effect of size on ear morphology and hearing performance has been explored in some mammals, anurans and lizards, much less is known about the scaling relationships for the single-ossicle, internally-coupled ears of birds. Using micro- and nano-CT scans of the tympanic middle and inner ears of 127 ecologically and phylogenetically diverse bird species, spanning more than 400-fold in head mass (2.3 to 950 g), we undertook phylogenetically-informed scaling analyses to test whether 12 morphological traits, of functional importance to hearing, maintain their relative proportions with increasing head mass. We then extended our analysis by regressing these morphological traits with measures of hearing sensitivity and range to better understand morphological underpinnings of hearing performance. We find that most

auditory structures scale together in equal proportions, whereas columella length increases disproportionately. We also find that the size of several auditory structures is associated with increased hearing sensitivity and frequency hearing limits, while head mass did not explain these measures. Although both birds and mammals demonstrate proportional scaling between auditory structures, the consequences for hearing in each group may diverge due to unique morphological predictors of auditory performance.

Keywords: allometry, hearing range, hearing sensitivity, impedance-matching, single ossicle ear

Highlights

- Scaling of ear morphology with increasing head mass may have implications for hearing performance
- In birds, most structures maintain equal proportions, but the columella becomes hyper-elongated
- The dimensions of several ear structures predict sensitivity and high frequency hearing limit
- Unlike mammals, head size and ossicle mass in birds do not appear to constrain high frequency hearing

Declarations of interest: none

1. Introduction

Auditory structures generally increase with overall animal body size, which can have size-related effects on hearing performance. One well documented relationship is the progression in hearing sensitivity towards lower frequencies with increasing body size. For example, in anurans (frogs) and lizards, larger body size is associated with lower frequencies of middle ear vibrations (Hetherington, 1992; Werner et al., 2002). In mammals, larger species have larger ear structures, several of which – tympanic membrane, columella footplate and cochlear labyrinth – are correlated with lower frequency hearing (Kirk and Gosselin-Ildari, 2009; Rosowski, 1994). Similarly, in birds, larger body size and longer basilar papillae (the primary hearing organ) correlate with a shift to lower frequency for best hearing sensitivity (Gleich et al., 2005), and a greater absolute mass of the middle ear ossicle predicts a lower frequency peak of middle ear vibration (Peacock et al., 2020).

Several anatomical mechanisms in the ear, as well as head dimensions, may contribute to the progression to lower frequency hearing with increasing body size. For example, the larger middle ear air cavities of larger animals can reduce middle ear stiffness, which can improve low frequency transmission through the ear (Mason, 2016). Larger ossicle mass can also create an inertia effect that limits high frequency transmission (Hemilä et al., 1995; Nummela, 1995). Larger tympanic membranes generally produce peak vibration amplitudes at lower frequencies than do smaller tympanic membranes (Hetherington, 1992; Werner et al., 2002), similar to how the area of a drum head affects its pitch (Plassmann and Brändle, 1992). In mammals, interaural-distances related to head size may also play a role in hearing limits; a comparative analysis revealed that high frequency hearing limit is inversely related to head size, likely to aid sound localization in smaller species (Heffner and Heffner, 2007).

In two non-mammalian groups – anurans and gecko lizards – positive associations have been reported between body size and either auditory sensitivity or middle ear vibration amplitudes, both at within- and between-species levels (Hetherington, 1992; James et al., 2021; Werner et al., 2008; Werner and Igić, 2002). By contrast, relationships between body size and auditory sensitivity are weaker in studies on mammals. For example, in 12 primates (species sizes ranging from lemurs to baboons), sizes of auditory structures or skull size are unrelated to hearing sensitivity in the frequency range of best sensitivity, although the size of some measures (tympanic membrane, columella footplate size) are linked to extended low

frequency hearing limits (Coleman and Colbert, 2010). Past studies that have attempted to link body size and hearing sensitivity may have failed to detect significant patterns due a narrow body size range.

The influence of body size on auditory structures and hearing performance can be assessed by scaling relationships in the middle and inner ear. In the middle ear, disproportionate scaling between structures (i.e., tympanic membrane-to-columella footplate area ratio, lever arms, conical protrusion) can affect size-dependent impedance matching and consequently hearing sensitivity. Disproportionate scaling may occur along the 'ideal-transformer' model of auditory function, which transmits air-borne sound into inner ear fluid vibrations via changes in impedance-matching mechanisms (Mason, 2016). These changes may involve variation in: (1) the ratio between the tympanic membrane and columella footplate area, (2) the first-order lever (in mammals) or second-order lever (in non-mammals) involving the auditory ossicle/s, (3) or the "curved lever" or catenary lever mechanism which increases pressure facilitated by the conical protrusion of the tympanic membrane (Manley, 1995; Saunders et al., 2000). In the inner ear, a disproportionate auditory endorgan size (measured as cochlear duct length) relative to skull size has been linked to hearing specialization across species of reptiles and birds (Walsh et al., 2009). Hearing sensitivity may also increase with body size due to disproportionate increase in cochlea size and number of hair cells (James et al., 2021; Werner et al., 2008).

By studying the scaling of auditory structures and the extent to which the dimensions of selected structures predict hearing performance, we can better understand how body size may influence hearing performance. Furthermore, different taxonomic groups might have evolved unique solutions to address potential size-dependent constraints on hearing, given that basic middle ear structure varies significantly among the major tetrapod groups (Mason and Farr, 2013). Examining deviations from proportional scaling between key structures in non-mammalian species can help identify major evolutionary divergence as well as detect possible convergence during the evolution of the tetrapod ear.

Birds provide an ideal group on which to examine the scaling relationships of a non-mammalian tympanic middle ear. First, their body size ranges from a few grams to over 100 kg, providing a broad base on which to detect potential effects of head and body size. Second, they provide an opportunity to examine scaling in a single ossicle, internally-coupled non-mammalian ear. Like that of other non-mammalian

tetrapods, the bird tympanic middle ear has a single ossicle, with a flexible cartilage component (extracolumella) that connects the ossicle (columella auris) to the tympanic membrane (Fig. 1). The tympanic membrane has an outward conical protrusion that adds a catenary lever mechanism, as well as a second-order lever mechanism that provides mechanical amplification (Gummer et al., 1989; Muyshondt and Dirckx, 2019).

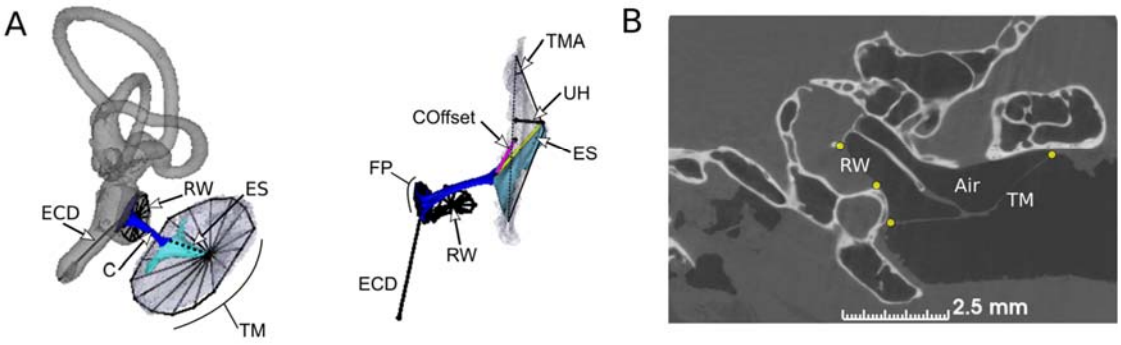

Fig. 1. Morphological measurements of auditory structures of the tympanic middle and inner ears of birds were made from (A) 3D micro- and nano-CT renderings and (B) 2D micro-CT slices oriented through the columella shaft. In 'A', the black lines show connection between points used for measurements (left shows rendering with labyrinth outlined; right shows rendering with labyrinth removed and oriented to highlight tympanic membrane measurements). In 'B', yellow dots depict the outline of the perimeter of tympanic membrane and round window. Abbreviations: Air is cranial air volume (mm^3), C is columella described in terms of columella length (mm) and columella volume (mm^3), COffset is columella offset from centroid of perimeter of tympanic membrane (mm), ECD is endosseous cochlear duct length (mm), ES is extrastapedius length (mm), FP is columella footplate area (mm^2), RW is round window area (mm^2), TM is tympanic membrane area (mm^2), TMA is tympanic membrane angle (degrees), UH is umbo height (mm).

In this study, we examine how selected auditory structures, of functional importance to hearing, change as a function of head mass in birds, and the extent to which certain morphological traits predict hearing sensitivity and range. We quantify the dimensions of auditory structures using micro- and nano-CT scans of the tympanic middle and inner ears from 127 species of ecologically and phylogenetically diverse birds spanning more than 400-fold in head mass. We then use phylogenetically-informed scaling analyses to test (1) whether the dimensions of

certain auditory structures maintain equal proportions among bird species, (2) how the dimensions of auditory structures vary as a function of increasing head mass, and (3) if the dimensions of certain auditory structures, once corrected for differences in head mass, are associated with metrics of hearing performance.

2. Materials and methods

2.1 Scaling relationships

We modelled scaling relationships using the equation:

$$y = ax^b, \quad (1.1)$$

where y and x are sizes of traits, and a and b define the elevation and shape of the power curve, respectively. Equation (1.1) can be rewritten as:

$$\log(y) = \log(a)+b*\log(x) \quad (1.2)$$

where b has the same value as in Equation (1.1) but now represents the slope of the linear relationship. When the size of two structures, having the same dimensions (e.g., length versus length), maintain equal proportion with each other, the relationship is termed isometric (slope = 1), whereas if the size of one structure varies disproportionately with respect to the other, either decreasing or increasing in relative size, it is termed hypo- (slope < 1; negative allometry) or hyperallometric (slope > 1; positive allometry), respectively (Fig 2A). However, when two structures, of differing dimensions are compared (e.g., length versus area), an isometric relationship will have a slope $\neq 1$ (defined in Fig 2B). In this study, the empirically observed slopes are compared against the expected isometric slopes based on geometric proportional scaling of the two dimensions.

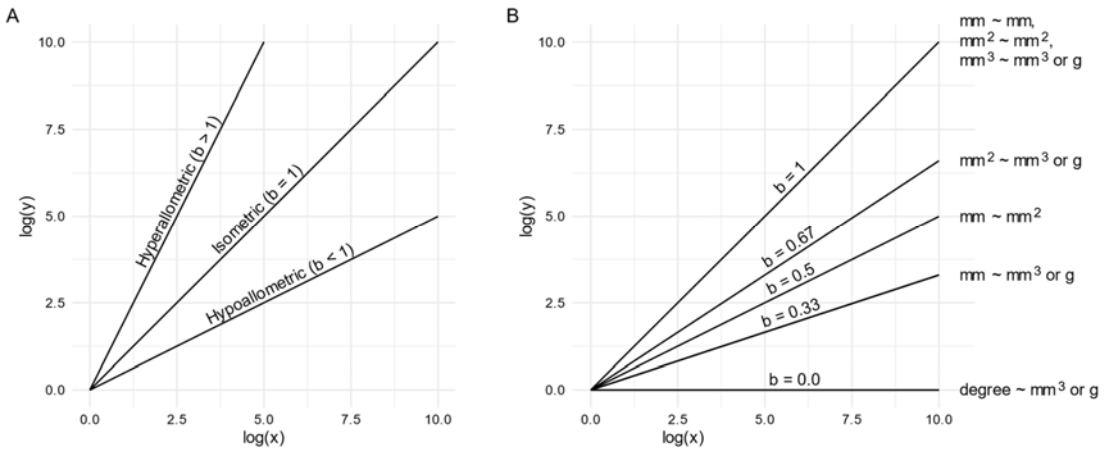

Fig 2. (A) Isometric, hypoallometric and hyperallometric relationships between two log-transformed morphological traits that have the same dimensions, e.g., length versus length. (B) Isometric relationships between two log-transformed morphological traits that have different dimensions, e.g., length versus area.

2.2 Species

Heads of naturally deceased adult birds, from 123 species (*N* = 130 specimens), were collected from several sources in South Africa, United Kingdom, and the Subantarctic Islands (specimen details and scan metadata in Supplemental material S1; CT scans available at MorphoSource repository, project entitled "Comparative studies of the bird ear", www.morphosource.org/projects/0000C1148?locale=en). A further four species (*N* = 5 specimens) were included from MorphoSource (details in Supplemental material S1). In total, the study used 127 species, comprising 26 orders, and spanning more than 400-fold in head mass (2.3 to 950 g) and 15,000-fold in body mass (7.3 g to 111 kg) (Fig. 3). Each specimen was carefully decapitated close to the base of the skull and heads were weighed with a digital balance (±0.01 g; SC-501A, American Weigh Scales, Atlanta, USA). Measurements from species for which multiple specimens were available were averaged to use a single value prior to analysis.

For each species, average adult body mass was taken from the literature (Dunning 2007). Where separate values for male and female body mass were available, we calculated an average because sex was often unknown in our specimens. In 13 species, head mass was unavailable (either because the digital scan data was obtained from MorphoSource or we did not have permission for

decapitation) and was estimated using a phylogenetic linear regression between skull width and head mass of 78 species of bird (R^2 = 0.88).

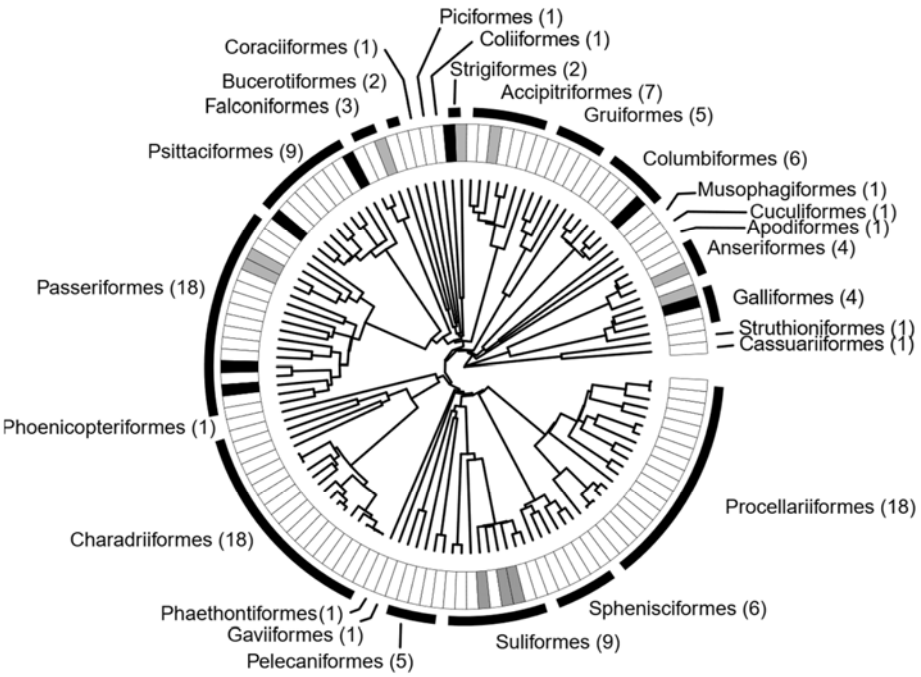

Fig. 3. Phylogeny of bird species included in the study. Bird orders are depicted by the outer black ring with the number of species sampled for each group in parentheses. The middle ring represents all the species used in analyses, with those for which we had audiograms for the same species (black) or for a congener (grey).

2.3 Morphological measurements

Morphological measurement of auditory structures of the middle and inner ear follow procedures described in (Zeyl et al., 2022) and its accompanying supplemental material. Briefly, heads were scanned with a nano-CT scanner (Nanotom S, General Electric, Wunstorf, Germany), or a micro-CT scanner (Phoenix v|tome|x L 240, General Electric) at the Central Analytical Facility, Stellenbosch University (du Plessis et al., 2016), or with a micro-CT scanner (XTH225 ST, Nikon, Tokyo, Japan) at the Cambridge Biotomography Centre, University of Cambridge. Morphological traits were measured in Volume Graphics VGSTUDIO MAX v. 3.2 and 3D Slicer v. 4.10.1, www.slicer.org (Fedorov et al., 2012). All custom codes used to make the measurements were developed in R v. 4.0.2 (R Core Team, 2020) and are available online (https://doi.org/10.5281/zenodo.4543752).

We took measurements for all three mechanisms of impedance-matching, namely the tympanic membrane-to-columella footplate area ratio, catenary lever (cone-shape), and second-order lever. The tympanic membrane, columella footplate, and round window areas were measured by tracing their perimeter and computing the sum of the triangles connecting perimeter points to a center point (Fig. 1; full details in Zeyl et al. 2022). The catenary lever was quantified with two measures of the conical protrusion of the tympanic membrane: (1) the average angle of conical protrusion of the tympanic membrane, measured for 16 perimeter points between the base plane of the tympanic membrane perimeter (plane of best fit through tympanic membrane perimeter points) and the umbo (i.e., the tip arising from the outward protrusion of the extrastapedius, the central process of the extracolumella), and (2) as the height of the umbo relative to the tympanic membrane base plane (Fig. 1). The second-order lever was quantified as the degree of offset of the columella tip from the center of the tympanic membrane (centroid of the perimeter points of the tympanic membrane). This is a proxy measure of the second-order lever mechanism, rather than a direct measurement of each lever arm. As the columella attaches closer to the centre of the tympanic membrane, it minimizes the lever action by reducing the differences in the length of lever arms (Manley, 1995; Saunders et al., 2000).

We also measured extrastapedius and columella lengths, cranial air volume, and endosseous cochlear duct length. Extrastapedius length was measured from the distal tip of the columella to the height of the umbo, and columella length was measured from the most distal point of the columella shaft to the footplate where the columella shaft inserts on the footplate. In birds, the air of the middle ear cavity is continuous with cranial air spaces and connects both ears (Larsen et al., 2016); therefore we measured the volume of all air behind the tympanic membrane in the caudal cranium, with a rostral delimitation occurring where the carotid arteries join together. We measured extrastapedius length and cranial air volume in the posterior portion of the cranium, continuous with the middle ear airspace, and measured columella size (length and volume). The endosseous cochlear duct length was measured as the distance from the centroid of the columella footplate (based on outline of the footplate perimeter) to the farthest point of the endosseous cochlear duct relative to the columella footplate (Fig. 1).

2.4 Audiogram measurements

We further compiled audiograms from published studies to obtain measures of hearing performance of the species studied (Table 1). Although hearing tests are available for many bird species, different experimental techniques contribute to additional variation of threshold values within and among species (Brittan-Powell et al., 2002; Crowell et al., 2016). Therefore, we restricted audiograms to those collected using behavioural training methods only (Gleich et al. 2005, Gleich and Langemann 2011). Auditory thresholds identified from behavioural responses elicited by a sound associated with a negative experience (e.g., an electric shock), are considered the 'gold standard' for hearing tests. In total, 17 of the 19 species from our anatomical dataset could be paired with appropriate audiogram data, either directly using the same species, or as a closely-related species of the same genus. In two instances, there were multiple congeners corresponding to one species with audiogram data: the great cormorant *Phalacrocorax carbo* had 3 congeners for which anatomical data were available and the hooded crow *Corvus cornix* had 2 congeners with data. For these species, values of congeners were averaged to a single value for use in analyses, resulting in a final sample size of 14 bird species.

Table 1. Bird species and references for audiograms taken from literature, and its relation to species for which morphological data (i.e., species with morphological data is a conspecific, congener, or no anatomical data) were measured in the current study. Species for which audiogram data were unavailable and thus substituted with a congener are identified.

Audiogram data					**Morphological data**		**Hearing limits (60 dB cut-off)**		**Hearing limits (35 dB cut-off)**	
Species	**Common name**	**Family**	**Order**	**Audiogram reference**	**Morphology data for this species**	**Congener(s) substitute**	**High frequency limit (Hz)**	**Low frequency limit (Hz)**	**High frequency limit (Hz)**	**Low frequency limit (Hz)**
Accipiter nisus	Eurasian sparrowhawk	Accipitridae	Accipitriformes	(Klump et al., 1986)	Congener	*Accipiter melanoleucus*	9901	NA	7590	271
Anas platryrhynchos	Mallard duck	Anatidae	Anseriformes	(Hill, 2017)	Congener	*Anas georgica georgica*	7677	66.3	6024	251
Aratinga canicularis	Orange fronted conure	Psittacidae	Psittaciformes	(Wright et al., 2003)	No	NA	6682	NA	4784.1	481
Aythya affinis	Lesser scaup	Anatidae	Anseriformes	(Crowell et al., 2016)	No	NA	6797	NA	4755	550
Bubo bubo	Eurasian eagle owl	Strigidae	Strigiformes	(Van Dijk, 1972)	Congener	*Bubo africanus*	NA	NA	NA	NA
Columba livia	Rock dove	Columbidae	Columbiformes	(Heffner et al., 2013)	Yes	NA	6463	40.4	4976	186
Corvus cornix	Hooded crow	Corvidae	Passeriformes	(Jensen and Klokker, 2006)	Congener	*Corvus albus, Corvus splendens*	7600	NA	6515	NA
Coturnix japonica	Japanese quail	Phasianidae	Galliformes	(Strawn and Hill, 2020)	No	NA	7117	59.1	6198	371

Cyanocitta cristata	Blue jay	Corvidae	Passeriformes	(Cohen et al., 1978)	No	NA	7894	NA	5227	580
Falco sparverius	American kestrel	Falconidae	Falconiformes	(Trainer, 1946)	Congener	*Falco rupicolus*	7650	NA	5870	339
Gallus domesticus	Domestic chicken	Phasianidae	Galliformes	(Hill et al., 2014)	Yes	NA	7285	10.0	6135	93.2
Melopsittacus undulatus	Budgerigar	Psittaculidae	Psittaciformes	(Heffner et al., 2016)	Yes	NA	7621	86.0	6462	218
Nestor notabilis	Kea parrot	Nestoridae	Psittaciformes	(Schwing et al., 2016)	No	NA	7371	328	4451	831
Nymphicus hollandicus	Cockatiel	Cacatuidae	Psittaciformes	(Okanoya and Dooling, 1987)	Yes	NA	6883	NA	5134	NA
Pavo cristatus	Indian peafowl	Phasianidae	Galliformes	(Heffner et al., 2020)	Congener	*Pavo muticus*	7211	28.0	5764	223
Phalacrocorax carbo	Great cormorant	Phalacrocoridae	Suliformes	(Maxwell et al., 2017)	Congener	*Phalacrocorax neglectus, Phalacrocorax lucidus, Phalacrocorax capensis*	NA	NA	3811	983
Serinus canaria	Canary	Fringillidae	Passeriformes	(Okanoya and Dooling, 1987)	Yes	N/A	NA	NA	7048	933
Taeniopygia guttata	Zebra finch	Estrildidae	Passeriformes	(Okanoya and Dooling, 1987)	Yes	N/A	7120	NA	5943	940
Tyto alba	Barn owl	Tytonidae	Strigiformes	(Dyson et al., 1998)	Yes	N/A	NA	NA	12067	NA

From each audiogram, we extracted four measures of hearing performance: best frequency (Hz), low and high frequency hearing limits (Hz), and lowest threshold of best sensitivity (decibel, dB) (Fig. 4). Best frequency refers to the frequency at which the lowest threshold occurs, and low and high frequency limits were the frequencies where audiograms crossed a cut-off sound level. We chose 60 and 35 dB SPL as cut-off sound levels. Although 60 dB is the typical sound level from a human perspective, and has traditionally been used in similar studies of mammals (Heffner et al. 2004; Heffner et al 2007), this cut-off reduced our sample size to $N = 5$ as several audiograms did not exceed this sound level. Therefore, a cut-off of 35 dB was also used to maximize available data. To find the precise frequencies at which the audiogram line crossed the cut-off sound levels, we performed a linear interpolation between tested frequencies using the 'approx' function in R. If the lowest or highest tested frequencies did not exceed the cut-off sound levels, they were removed from the analysis. Best sensitivity was defined as the minimum sound level present in the audiogram. Summary figures depicting the metrics for each species can be seen in Supplemental material S2.

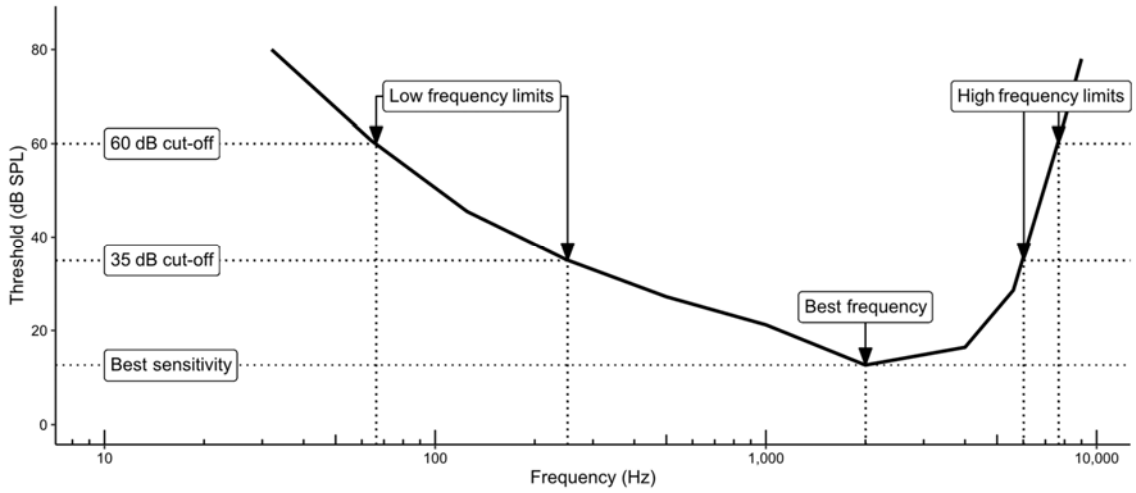

Fig 4. Example of an audiogram (mallard duck, *Anas platyrhynchos*; taken from (Hill, 2017)) indicating the four extracted measures of hearing performance: best frequency (Hz), low and high frequency hearing limits (Hz) at 60 and 35 dB cut-off levels, and best sensitivity (i.e., lowest threshold in dB).

2.5 Statistical analyses

We used phylogenetically-informed regressions of log-transformed variables to test whether the dimensions of certain auditory structures maintain equal

proportions among bird species. To achieve this, scaling relationships between auditory structures were separated into three categories: (1) those related to impedance-match function of the middle ear (tympanic membrane area ~ columella footplate area, round window area ~ footplate area, columella offset distance ~ tympanic membrane area, umbo height ~ tympanic membrane area, tympanic membrane angle ~ tympanic membrane area), (2) those related to the stiffness of the middle ear due to relative lengths of the ossicle/cartilage components (extrastapedius length ~ columella length), and (3) those related to columella morphology and its size relative to middle ear area openings (columella length ~ columella volume, columella length ~ columella footplate area, footplate area ~ columella volume, and tympanic membrane area ~ columella volume). Next, we assessed how the dimensions of all 12 auditory structures vary with head mass. Lastly, we tested whether the dimensions of all 12 auditory structures, once corrected for differences in head mass, and head mass itself, are associated with metrics of hearing performance.

Statistical analyses were conducted in R v. 4.0.2, and the codes and data are available online (https://zenodo.org/record/7317140#.Y3E8H3bMLx4). We used phylogenetic generalised least squares (PGLS) regressions, which account for the non-independence of data points due to phylogenetic relatedness by incorporating information from the phylogenetic tree structure. The backbone of the phylogeny was taken from Prum et al. (2015) and combined with a recent species-level phylogeny from birdtree.org (see data in repository https://zenodo.org/record/6972659#.YvB5q3bMLx4), using the R code and methods described in the supplemental material of Cooney et al., 2017. Goodness of fit was assessed with the adjusted R^2 (hereafter simply R^2) and Pagel's lambda was computed using maximum likelihood to assess the degree of phylogenetic signal. Deviation from isometry was tested by examining whether the exponent's 95% confidence range included the expected geometric scaling exponent (i.e., isometry), or if it fell above (i.e., hyperallometry) or below (i.e., hypoallometry) the confidence range.

PGLS regressions were also used to relate morphological traits, corrected for head mass, to audiogram hearing range and sensitivity thresholds. To generate trait values independent of head mass, we used the residuals of the PGLS regression between each auditory structure and head mass. Associations between audiogram metrics were determined using Pearson correlations. Best frequency, low frequency

hearing limit, and high frequency hearing limit were log-transformed prior to applying the PGLS regressions. PGLS diagnostics including normality and homoscedasticity of residuals were checked for all models and conformed reasonably well. Slope estimates were compared to expected geometric scaling exponents (scaling analyses) and to a slope of zero (audiogram analyses) using two-tailed t-tests and p-values evaluated with an alpha level of 0.05. Summary statistics are mean ± s.e.m unless otherwise indicated.

3. Results

3.1 Scaling between auditory structures

The tympanic membrane area scaled isometrically (i.e., in equal proportions) with the footplate area, umbo height, and the columella offset distance (Table 2). The average tympanic membrane-to-columella footplate area ratio was 24.5 ± 1.1 and the average tympanic membrane angle was 18.2 ± 1.2 degrees and the latter varied considerably for a given tympanic membrane area (Table 2). The round window and columella footplate areas scaled isometrically with each other (Table 2), with the round window area being on average 3.0 ± 1.1 times larger than the footplate area.

Extrastapedius length was hypoallometric relative to columella length as the size of both structures increased (Table 2). A columella equal to the first quartile of length measurements would have an extrastapedius 0.51-times as long as the columella, whereas a columella in the third quartile would have an extrastapedius 0.77-times as long. Columella length was hyperallometric relative to other measures of columella size – columella volume and columella footplate area. The two major input areas of the middle ear, columella footplate area and tympanic membrane area, were hypoallometric relative to columella volume. Scatterplots of all relationships described above are available in Supplemental material S3.

Table 2. PGLS models testing the relationship between the sizes of auditory structures of birds. The expected isometric slope (exponent), obtained if the sizes of the two log-transformed structures vary in geometric proportion to each other, is compared to the observed slope derived from the PGLS model (lower and upper 95% confidence intervals in parentheses). “Hyper” refers to hyperallometry or positive allometry (size of trait A is disproportionately greater than trait B with increasing size), “Hypo” is hypoallometry or negative allometry (size of trait is disproportionately smaller than trait B with increasing size) and “Iso” is isometry (size of trait A increases at same rate as size of trait B). Pagel’s lambda (λ) describes the degree of phylogenetic signal. Abbreviations: CL is columella length (mm), COffset is columella offset distance from centroid of perimeter of tympanic membrane (mm), CV is columella volume (mm^3), ES is extrastapedius length (mm), FP is columella footplate area (mm^2), RW is round window area (mm^2), TM is tympanic membrane area (mm^2), TMA is tympanic membrane angle (degrees), UH is umbo height (mm). Morphological structures are log-transformed in prior to analyses.

Category	Dependent variable	Independent variable	Expected isometric slope	Observed slope (95%CI)	Observed scaling	R^2	P value	λ
Impedance match	TM	FP	1.00	1.00 (0.88, 1.12)	Iso	0.71	1.00	0.54
Impedance match	RW	FP	1.00	0.89 (0.78, 1.00)	Iso	0.67	0.056	0.77
Impedance match	COffset	TM	0.50	0.47 (0.40, 0.54)	Iso	0.57	0.42	0.50
Impedance match	UH	TM	0.50	0.47 (0.38, 0.56)	Iso	0.45	0.52	0.38
Impedance match	TMA	TM	0.00	-0.02 (-0.11, 0.07)	Iso	-0.01	0.71	0.34
Stiffness	ES	CL	1.00	0.54 (0.45, 0.63)	Hypo	0.50	< 0.001	0.79
Columella morphology	CL	CV	0.33	0.44 (0.41, 0.47)	Hyper	0.85	< 0.001	0.61
Columella morphology	CL	FP	0.50	0.74 (0.65, 0.82)	Hyper	0.69	< 0.001	0.89
Columella morphology	FP	CV	0.67	0.43 (0.38, 0.48)	Hypo	0.69	< 0.001	0.70
Columella morphology	TM	CV	0.67	0.47 (0.40, 0.54)	Hypo	0.56	< 0.001	0.75

3.2 Scaling of auditory structures with head mass

Head mass scaled hypoallometrically with increasing body mass (slope: 0.63 ± 0.04), meaning larger birds have relatively smaller heads. Furthermore, most structures scaled hypoallometrically with increasing head mass (Table 3), meaning larger heads also tend to have relatively smaller auditory structures. Three exceptions were columella length, which scaled hyperallometrically with head mass, and cranial air volume and tympanic membrane-to-columella footplate area ratio, which both scaled isometrically with head mass (Table 3). Columella length and volume showed the strongest relationship with head mass (R^2 =0.81 and 0.78, respectively). Impedance-matching metrics such as the columella offset, umbo height, tympanic membrane angle and the tympanic membrane-to-columella footplate area ratio, lacked a strong relationship with head mass (R^2 ranged from 0.01-0.36) (Supplemental material S3).

Table 3. PGLS models testing the relationship between the sizes of auditory structures and head mass of birds. The expected isometric slope, obtained if the size of the structure varies in direct geometric proportion with head mass, is compared to the observed exponent derived from the PGLS model (lower and upper 95% confidence intervals in parentheses). "Hyper" refers to hyperallometry or positive allometry, "Hypo" is hypoallometry or negative allometry, and "Iso" is isometry. Pagel's lambda (λ) describes the degree of phylogenetic signal. Abbreviations: Air is cranial air volume (mm^3), CL is columella length (mm), COffset is columella offset from centroid of perimeter of tympanic membrane (mm), CV is columella volume (mm^3), ECD is endosseous cochlear duct length (mm), ES is extrastapedius length (mm), FP is columella footplate area (mm^2), RW is round window area (mm^2), TM is tympanic membrane area (mm^2), TMA is tympanic membrane angle (degrees), TM_FP is tympanic membrane-to-columella footplate area ratio, UH is umbo height (mm). Morphological structures are log-transformed prior to analyses.

Category	Dependent	Expected isometric slope	Observed slope (95%CI)	Observed scaling	R^2	P value	λ
Columella size	CL	0.33	0.41 (0.36, 0.44)	Hyper	0.81	< 0.001	0.75
Columella size	CV	1.00	0.85 (0.76, 0.92)	Hypo	0.78	< 0.001	0.48

Category	Dependent	Expected isometric slope	Observed slope (95%CI)	Observed scaling	R^2	P value	λ
Auditory endorgan length	ECD	0.33	0.22 (0.20, 0.24)	Hypo	0.75	< 0.001	0.91
Input/output areas	FP	0.67	0.40 (0.35, 0.46)	Hypo	0.62	< 0.001	0.85
Input/output areas	RW	0.67	0.42 (0.36, 0.48)	Hypo	0.60	< 0.001	0.77
Input/output areas	TM	0.67	0.43 (0.36, 0.50)	Hypo	0.51	< 0.001	0.83
Stiffness	Air	1.00	0.98 (0.82, 1.14)	Iso	0.56	0.81	0.79
Stiffness	ES	0.33	0.24 (0.20, 0.28)	Hypo	0.48	< 0.001	0.82
Impedance matching	COffset	0.33	0.24 (0.18, 0.30)	Hypo	0.36	0.002	0.70
Impedance matching	UH	0.33	0.16 (0.09, 0.23)	Hypo	0.13	< 0.001	0.66
Impedance matching	TMA	0.00	-0.07 (-0.12, -0.02)	Hypo	0.05	0.009	0.25
Impedance matching	TM_FP	0.00	0.05 (0.00, 0.11)	Iso	0.01	0.100	0.51

3.3 Relationships with audiograms

Available audiograms included species with average body mass ranging from 24.4 to 4149 g. Among the 14 bird species with audiograms and associated morphological data, four audiograms did not reach the 35 dB cut-off for the low frequency limit, resulting in *N* = 10, and one audiogram did not reach the 35 dB cut-off for the high frequency limit, resulting in *N* = 13 (Table 1, Fig. S3). At a 60 dB cut-off, nine audiograms did not reach the low frequency cut-off limit, resulting in *N* = 5, and four audiograms did not reach the high frequency cut-off limit, resulting in *N* = 10 (Table 1, Fig. S3).

The best sensitivity covered a range of 41 dB and averaged 6.53 dB (± 2.64), and the best frequency averaged 2.4 kHz (± 0.2). Mean low and high frequencies

were 483Hz (±70) and 6042 Hz (±408), respectively, at the 35 dB cut-off level, and 88.2 Hz (±24.9) and 7418 Hz (±183), respectively, at the 60 dB cut-off level. Using the 35 dB cut-off, the best sensitivity was highly negatively correlated with high frequency hearing limit ($r = -0.79$, $P < 0.001$) and positively correlated with low frequency hearing limit ($r = 0.58$, $P = 0.021$). High and low frequency hearing limits were not correlated ($r = -0.35$, $P = 0.20$) and the best frequency showed a significant positive correlation with low frequency hearing limit ($r = 0.65$, $P = 0.009$). At the 60 dB cut-off, only the significant negative correlation between best sensitivity and high frequency hearing limit remained ($r = -0.62$, $P = 0.014$).

Best sensitivity was negatively related to the relative size of several auditory structures, including impedance matching metrics, measures of stiffness (cranial air and extrastapedius length), areas of sound input/output (round window, footplate, and tympanic membrane areas), auditory endorgan length (endosseous cochlear duct length), and columella volume (Table 4, Supplemental material S4). Three of the four impedance-matching structures (tympanic membrane area, columella offset distance and umbo height) adjusted for size were negatively related to best sensitivity (Table 4; Supplemental material S4), but no relationship was found between best sensitivity and the size-adjusted tympanic membrane-to-columella footplate area ratio ($P = 0.16$). Best frequency was negatively related with head mass (Table 4).

At the 35 dB cut-off, there were no significant anatomical predictors of low frequency hearing limit. High frequency hearing limit was positively related to the same size-adjusted structures that predicted best sensitivity, except columella volume and round window area (Table 4). Larger size-adjusted tympanic-membrane-to-footplate area ratio was associated with greater high frequency hearing limit (Table 4). At the 60 dB cut-off, a low frequency hearing limit was negatively related to several structures – greater tympanic membrane angle, extrastapedius length, endosseous cochlear duct length, and columella volume – but there were no significant relationships with high frequency limits (Table 4, Supplemental material S4).

Relationships between audiogram metrics and absolute size of auditory structures (i.e., unadjusted for head size) were mostly consistent with relationships obtained from size-adjusted data with a few exceptions (Supplemental material S4). Predictors of best sensitivity remained the same. At the 35 dB cut-off, four out of the nine variables predicting high frequency hearing limit remained significant (i.e.,

tympanic membrane angle, tympanic membrane-to-columella footplate area ratio, umbo height, and columella offset). In addition, larger structures such as columella offset, extrastapedius length, cranial air, and columella footplate area predicted reduced low frequency limits. At the 60 dB cut-off, all results were similar to size adjusted analyses except that columella offset was also negatively related to low frequency hearing limit. Best frequency was predicted head mass and columella footplate area.

Table 4. PGLS models testing the relationship between the sizes of auditory structures independent of head mass (residuals of a PGLS regression between each measure and head mass) and audiogram metrics (high and low frequency limits, best frequency, best sensitivity). Only significant predictors are presented. Models where head mass alone is a significant predictor are also shown. Abbreviations: Air is cranial air volume (mm^3), CL is columella length (mm) and CV is columella volume (mm^3), COffset is columella offset from centroid of perimeter of tympanic membrane (mm), ECD is endosseous cochlear duct length (mm), ES is extrastapedius length (mm), FP is columella footplate area (mm^2), RW is round window area (mm^2), TM is tympanic membrane area (mm^2), TMA is tympanic membrane angle (degrees), TM_FP is tympanic membrane-to-columella footplate area ratio, UH is umbo height (mm).

Audiogram metric	Category	Predictor	Estimate (95% CI)	R^2	P value	λ
Best sensitivity (dB)	Impedance match	Residual UH	-19.6 (-29.5, -9.7)	0.52	0.0022	0.79
Best sensitivity (dB)	Impedance match	Residual TMA	-39.2 (-60.8,-17.6)	0.47	0.0039	0.96
Best sensitivity (dB)	Impedance match	Residual Coffset	-21.8 (-34.4, -9.2)	0.45	0.0054	0.43
Best sensitivity (dB)	Stiffness	Residual Air	-11.7 (-18.1, -5.2)	0.47	0.0041	0.01
Best sensitivity (dB)	Stiffness	Residual ES	-19.3 (-34.5, -4.1)	0.29	0.028	1.0
Best sensitivity (dB)	Input/output areas	Residual RW	-21.4 (-31.7,-11.1)	0.55	0.0015	0.01
Best sensitivity (dB)	Input/output areas	Residual TM	-16.8 (-25.7, -7.9)	0.50	0.0029	0.38
Best sensitivity (dB)	Input/output areas	Residual FP	-20.3 (-31.7, -8.9)	0.46	0.0046	0.01
Best sensitivity (dB)	Auditory endorgan length	Residual ECD	-38.6 (-57.5, -19.7)	0.54	0.0017	0.01
Best sensitivity (dB)	Columella size	Residual CV	-14.9 (-22.8, -7.0)	0.49	0.003	0.01
High frequency limit (Hz) (35 dB cut-off)	Impedance match	Residual Coffset_	0.52 (0.27, 0.78)	0.54	0.0024	0.01

High frequency limit (Hz) (35 dB cut-off)	Impedance match	Residual UH	0.43 (0.20, 0.67)	0.51	0.0037	0.01
High frequency limit (Hz) (35 dB cut-off)	Impedance match	Residual TM_FP	0.72 (0.27, 1.2)	0.42	0.01	1.0
High frequency limit (Hz) (35 dB cut-off)	Impedance match	Residual TMA	0.71 (0.16, 1.3)	0.31	0.027	0.01
High frequency limit (Hz) (35 dB cut-off)	Stiffness	Residual Air	0.26 (0.14, 0.38)	0.58	0.0015	0.01
High frequency limit (Hz) (35 dB cut-off)	Stiffness	Residual ES	0.40 (0.067, 0.73)	0.28	0.035	1.0
High frequency limit (Hz) (35 dB cut-off)	Input/output areas	Residual TM	0.38 (0.18, 0.58)	0.53	0.0028	0.01
High frequency limit (Hz) (35 dB cut-off)	Input/output areas	Residual FP	0.4 (0.086, 0.71)	0.29	0.034	0.01
High frequency limit (Hz) (35 dB cut-off)	Auditory endorgan length	Residual ECD	0.77 (0.28, 1.26)	0.42	0.0098	0.79
Low frequency limit (Hz) (60 dB cut-off)	Impedance match	Residual TMA	-3.5 (-5.34, -1.7)	0.76	0.035	0.01
Low frequency limit (Hz) (60 dB cut-off)	Stiffness	Residual ES	-4.6 (-6.8, -2.4)	0.82	0.022	1.0
Low frequency limit (Hz) (60 dB cut-off)	Auditory endorgan length	Residual ECD	-4.6 (-6.756, -2.4)	0.79	0.027	1.0
Low frequency limit (Hz) (60 dB cut-off)	Columella size	Residual CV	-1.3 (-2.045, -0.55)	0.71	0.045	1.0
Best Frequency (Hz)	Head size	HM	-0.26 (-0.460, -0.060)	0.30	0.0256	0.01

4. Discussion

4.1 Scaling relationships

The auditory structures of birds involved in impedance matching maintained their proportions with increasing tympanic membrane size. Both the columella footplate area and the tympanic membrane area scaled together in equal proportions, and the lever metrics (umbo height and the columella offset) were isometric with the tympanic membrane area. Other auditory structure scaling studies in birds have found either isometry between oval window area and tympanic membrane area (Peacock et al., 2020) or, in a smaller sample of 35 species, a

hypoallometry of oval window area with respect to tympanic membrane area (Nummela 1997). In a broader comparative context, our observed isometry is similar to patterns found in mammals, with lever ratios and tympanic membrane scaling isometrically (Hemilä et al., 1995). By contrast, allometric scaling between impedance matching structures occurs in geckos; an interspecific study revealed a decrease in lever action in larger species, combined with an increase in tympanic membrane-to-columella footplate area ratio and increasing sensitivity (Werner and Igić, 2002).

The increase of columella offset accompanying increases in tympanic membrane area in birds suggests that the distal tip of the columella remains positioned near the margin of the tympanic membrane. This orientation would be essential to maintain a second-order lever with increasing tympanic membrane size, because it would keep the short arm of the second-order lever (i.e., from columella tip to the margin of the tympanic membrane) small. However, the columella offset distance is a proxy measure, not a direct quantification of lever arms. Morphological definitions of the second-order lever arms in birds have varied among studies (Claes, 2018; Mason and Farr, 2013). Since there are two processes of the extracolumella (the infrastapedius and the suprastapedius) inserting near the tympanic membrane margin, the fulcrum may occur somewhere between the two processes, or alternatively around a single process (the infrastapedius).

We highlight a large round window relative to the footplate (and in turn the oval window) in birds. Like middle ear impedance structures, the columella footplate area and the round window maintained equal proportions across scale. The round window area of birds is approximately 3-times larger relative to the columella footplate compared to, for example humans, where oval windows (occupied primarily by the footplate) are estimated to be near 1.5-times larger [oval window of 3 mm^2 (Zdilla et al., 2018), round window of 2 mm^2 (Atturo et al., 2014)]. To our knowledge this is the first comparative quantification of the round window in birds. A relatively larger round window may serve to lower inner ear impedance, an idea that is consistent with the observation of a low inner ear impedance in the ostrich compared to mammals (Muyshondt et al., 2016).

The functional significance of the hyper-elongation of the columella requires further investigation, but we propose some possibilities. The audiogram data did not support a major role for columella length affecting hearing abilities, which could indicate either that columella hyper-elongation does not impact auditory performance,

or that it serves to maintain auditory function across size. Since the extracolumella is made of flexible cartilage, a disproportionate elongation of this structure would likely result in more middle ear flexibility and absorption of more vibrational energy, making the mechanical transduction less effective, particularly at higher frequencies (Mason and Farr, 2013). As columella length outpaces columella volume, it could distribute the mass across the columella, lowering the cross-sectional density of the columella, and thus reducing inertia and potentially maintaining high frequency hearing in larger birds. In mammals, where columella mass scales isometrically with tympanic membrane area (Nummela, 1995), columella mass in larger species confers an inertia effect which can be used to predict high frequency hearing limits (Hemilä et al., 1995). In birds, columella mass was previously found to scale isometrically with tympanic membrane area (Nummela 1997), but we found that tympanic membrane area was hypoallometric relative to columella volume. With the assumption that columella volume is a good proxy for mass, a columella mass that scales in a hypoallometrically manner relative to tympanic membrane area would likely elicit in an even greater potential for a columella inertia effect in larger species. However, columella volume was not related to high frequency hearing limit in our data, suggesting that columella inertia is not a major factor in limiting high frequency hearing in birds.

Columella hyper-elongation as a function of head size might be a more widespread feature in single-ossicle ears, since in addition to our comparative study in birds, it has been observed in lizards. In a 14-species comparison of geckos, the columella is disproportionately longer than the extracolumella in larger individuals (Table 2), and both inter- and intra-species analyses show that larger individuals have a middle ear with lower ‘percent cartilage’ (extracolumella length/(extracolumella length + columella length) (Werner and Igić, 2002). A recent scaling study of birds found that columella length increases faster than columella mass (Peacock et al., 2020). In mammals, by contrast, the masses of the three ear bones (incus, malleus and stapes) maintain isometric proportions together across a wide size range of species (Nummela, 1995).

The hypoallometry we found between most auditory structures and head mass follows findings related to head size in other studies on birds (Peacock et al., 2020; Nummela 1997) and mammals (using skull mass; Nummela, 1995; Nummela and Sánchez-Villagra, 2006). Cranial air volume is likely isometric with head mass because the pneumatic airspaces scale directly with covering cranial bone. In very

small birds (e.g., sunbirds), the ear may have to be a minimum size to function optimally while in large birds, equal proportions are not required to preserve hearing.

Among auditory structures, columella length and volume showed the tightest relationship with head mass, whereas impedance-matching metrics (*viz*. columella offset, umbo height, tympanic membrane angle, and the tympanic membrane-to-columella footplate area ratio) were least strongly linked with head mass (R^2 all less than 0.36). Similarly, in mammals, the tympanic membrane-to-stapes footplate area ratio is also variable across species and independent of body size (Mason 2001) and skull size (Nummela 1995). This suggests that these middle traits are more anatomically flexible and may be related to life history differences between species in the need for sensitive hearing or they are not tightly influenced by size or phylogeny.

4.2 Auditory morphology and hearing performance

The sizes of several auditory structures predicts both best sensitivity and high frequency hearing limit. In contrast, head mass only predicts best frequency, highlighting the benefit of measuring ear structures to understand hearing performance.

Best sensitivity

Several anatomical mechanisms may underlie the relationship between scaling of the ear and best sensitivity. First, larger tympanic membrane and footplate areas have better membrane mobility – larger tympanic membranes may have a proportionally larger effective area than smaller tympanic membranes, since some thickening of tissues occurs at the margins of the tympanic membrane and may be less responsive to vibration. Work on anurans and geckos support this hypothesis, where larger tympanic membrane areas can have greater peak vibration amplitude, and are positively associated with auditory sensitivity (Fox, 1995; Hetherington, 1992; Werner et al., 2008). Another possibility, supported by the positive relationship between best sensitivity and umbo height, tympanic membrane area, and columella offset, is that larger ears exhibit greater lever action and consequently achieve greater impedance matching (Table 3). Theoretically, an increasing columella offset from the centre of the tympanic membrane could maintain and potentially be associated with an increase second-order lever action in larger tympanic membranes (Manley, 1995). A third possibility, supported by the positive relationship between best sensitivity and endosseous cochlear duct length, is that sensitivity may increase

with a relatively larger cochlea with a higher number of hair cells (James et al., 2021; Werner et al., 2008). This result supports the common use of endosseous cochlear duct length scaled to head size (length) as a measure of auditory specialization broadly among birds, reptiles, and dinosaurs fossils (Choiniere et al., 2021; Walsh et al., 2009).

Although our metrics pertaining to lever action could be used to predict best sensitivity, tympanic membrane-to-columella footplate area ratio was not, despite the latter metric typically assumed to be the primary determinant of impedance matching (Christensen-Dalsgaard and Manley, 2013). A difference in area between the tympanic membrane and the columella footplate is required for the 'ideal transformer' model of middle ear function, but several studies have found that this anatomical metric has limited use as a predictor of auditory sensitivity (Coleman and Colbert, 2010; Rosowski and Graybeal, 1991; Rosowski, 1994), because it overlooks the influence of structural mass and stiffness (Mason, 2016; Mason and Farr, 2013).

Hearing limits

Unlike comparative studies done on mammals, where increases in head size (Heffner, 2004) and columella mass (Hemilä et al., 1995) can predict a lowering of high frequency hearing limit, we did not detect a similar relationships based on our measures of head mass and columella volume. This suggests that in birds, unlike in mammals, the high frequency hearing limit is not constrained by head size or columella inertia. The lack of a relationship between head size and high frequency hearing limit in birds could be due to the effects of internally coupled ears, which confer a larger 'physiological head size' to birds than similarly sized mammals. Internally coupled ears should allow sound localization at low frequencies without the need to depend on sensitivity to high frequencies (which generate larger interaural level differences between the ears than lower frequencies) (Heffner, 2004; Köppl, 2009). Therefore, relative to small mammals, the selective pressure on high frequency hearing in small birds and other non-mammalians that also have internally coupled ears (e.g., lizards) may be lower.

A subset of the anatomical structures that enhanced best sensitivity also significantly extended low and high frequency hearing limits, suggesting that an increasing size of certain morphological structures in the middle and inner ear can simultaneously increase hearing limits and best sensitivity. Endosseous cochlear duct length, extrastapedius length, and tympanic membrane angle were associated

with extension of both low and high frequency hearing limits, though at different cut-off levels, whereas tympanic membrane-to-columella footplate area ratio and columella volume were exclusively associated with high and low frequency limits, respectively. However, given that our strict cut-off sound levels resulted in small sample sizes, our results on hearing limits may be influenced by low statistical power or potentially non-representative samples. Therefore, data from additional audiograms are urgently needed and will help to further resolve which structures are likely predictive of hearing limits.

The associations between best sensitivity (in dB) and both low and high frequency hearing limits also support the notion that traits that increase hearing sensitivity at best frequencies could confer an increase in overall hearing range. High frequency hearing limit is strongly correlated with sensitivity, and the high frequency side of the audiogram is strongly conserved in non-owl species, whereas the low frequency is less steep and more variable among species (Gleich and Langemann 2011). The absence of correlation between low and high frequency hearing limits suggest a lack of trade-off between low and high frequency hearing specialization in birds.

4.3 Conclusion

Here we provide the first analysis of scaling relationships of auditory structures of birds and their relationship to hearing performance, using a large, phylogenetically and ecologically diverse group of birds with a wide head and body size range. Similar to mammals, the auditory structures of birds are hypoallometric relative to head mass, but relationships among structures were generally isometric, with the exception of the hyper-elongation of the columella. The relationships between sizes of ear structures and hearing performance, however, revealed some clear deviations from mammals. In birds, there was no evidence for constraints on high frequency hearing limits related to head or columella size. The relative size of auditory structures, but not head size, are predictive of audiogram metrics, particularly best sensitivity and hearing limits, highlighting the importance of examining these structures to assess hearing performance.

Acknowledgements

We thank the many researchers, conservation agencies, and rehabilitation centers for assistance with providing bird heads, including SANCCOB, British Antarctic Survey, Fitzpatrick Institute, Nelson Mandela University. We specifically thank Maëlle Connan, Thomas A. Clay, Samantha C. Patrick, Richard A. Phillips, Pierre A. Pistorius, Peter G. Ryan, Jacques Scheepers and Albert Snyman for facilitating specimen collections. We acknowledge Ket Smithson for conducting CT scans at the University of Cambridge and Muofhe Tshibalanganda for assistance with scans at University of Stellenbosch. Deceased bird head specimens in South Africa were collected under permit numbers CN44-59-11521 (CapeNature) and RES2020/81 (DEA). Specimen collection at South Georgia was carried out with permission of the Government of South Georgia and the South Sandwich Islands, and collection from Marion Island with permission from South African National Antarctic Programme (#110738 and #093071). All scans are openly available in the MorphoSource repository, as part of Zeyl et al. 2022 and the project entitled “Comparative studies of the bird ear”.

Funding

This research was supported by a Human Frontier Science Program Young Investigator Grant (SeabirdSound; RGY0072/2017).

Author contributions

JNZ – Conceptualization, Data collection, Formal analysis, Original Draft, Review & Editing

SCT – Conceptualization, Formal analysis, Review & Editing

EPS – Conceptualization, Formal analysis, Review & Editing

RJ – Formal analysis, Review & Editing

References

Atturo, F., Barbara, M., Rask-Andersen, H., 2014. Is the Human Round Window Really Round? An Anatomic Study With Surgical Implications. Otol. Neurotol. 35, 1354–1360. https://doi.org/10.1097/MAO.0000000000000332

Brittan-Powell, E.F., Dooling, R.J., Gleich, O., 2002. Auditory brainstem responses in adult budgerigars (*Melopsittacus undulatus*). J. Acoust. Soc. Am. 112, 999–1008. https://doi.org/10.1121/1.1494807

Choiniere, J.N., Neenan, J.M., Schmitz, L., Ford, D.P., Chapelle, K.E.J., Balanoff, A.M., Sipla, J.S., Georgi, J.A., Walsh, S.A., Norell, M.A., Xu, X., Clark, J.M., Benson, R.B.J., 2021. Evolution of vision and hearing modalities in theropod dinosaurs. Science 372, 610–613. https://doi.org/10.1126/science.abe7941

Christensen-Dalsgaard, J., Manley, G.A., 2013. The Malleable Middle Ear: An Underappreciated Player in the Evolution of Hearing in Vertebrates, in: Köppl, C., Manley, G.A., Popper, A.N., Fay, R.R. (Eds.), Insights from Comparative Hearing Research, Springer Handbook of Auditory Research. Springer New York, pp. 157–191.

Claes, R., 2018. Understanding functioning and evolution of bird middle ear mechanics: a functional morphological analysis (PhD Thesis). University of Antwerp.

Claes, R., Muyshondt, P.G.G., Dirckx, J.J.J., Aerts, P., 2018. Deformation of avian middle ear structures under static pressure loads, and potential regulation mechanisms. Zoology 126, 128–136. https://doi.org/10.1016/j.zool.2017.11.003

Cohen, S.M., Stebbins, W.C., Moody, D.B., 1978. Audibility Thresholds of the Blue Jay. The Auk 95, 563–568. https://doi.org/10.1093/auk/95.3.563

Coleman, M.N., Colbert, M.W., 2010. Correlations between auditory structures and hearing sensitivity in non-human primates. J. Morphol. 271, 511–532. https://doi.org/10.1002/jmor.10814

Cooney, C.R., Bright, J.A., Capp, E.J.R., Chira, A.M., Hughes, E.C., Moody, C.J.A., Nouri, L.O., Varley, Z.K., Thomas, G.H., 2017. Mega-evolutionary dynamics of the adaptive radiation of birds. Nature 542, 344–347. https://doi.org/10.1038/nature21074

Crowell, S.E., Wells-Berlin, A.M., Therrien, R.E., Yannuzzi, S.E., Carr, C.E., 2016. In-air hearing of a diving duck: A comparison of psychoacoustic and auditory brainstem response thresholds. J. Acoust. Soc. Am. 139, 3001–3008. https://doi.org/10.1121/1.4948574

du Plessis, A., le Roux, S.G., Guelpa, A., 2016. The CT Scanner Facility at Stellenbosch University: An open access X-ray computed tomography laboratory. Nucl. Instrum. Methods Phys. Res. Sect. B Beam Interact. Mater. At. 384, 42–49. https://doi.org/10.1016/j.nimb.2016.08.005

Dunning Jr, J.B., 2007. CRC handbook of avian body masses. CRC press.

Dyson, M.L., Klump, G.M., Gauger, B., 1998. Absolute hearing thresholds and critical masking ratios in the European barn owl: a comparison with other owls. J. Comp. Physiol. A 182, 695–702. https://doi.org/10.1007/s003590050214

Fedorov, A., Beichel, R., Finet, J., Fillion-Robin, J.-C., Pujol, S., Bauer, C., Jennings, D., Fennessy, F., Sonka, M., Buatti, J., Aylward, S., Miller, J.V., Pieper, S., Kikinis, R., 2012. 3D Slicer as an image computing platform for the Quantitative Imaging Network. Magn. Reson. Imaging, Quantitative Imaging in Cancer 30, 1323–1341. https://doi.org/10.1016/j.mri.2012.05.001

Fox, J.H., 1995. Morphological Correlates of Auditory Sensitivity in Anuran Amphibians. Brain. Behav. Evol. 45, 327–338. https://doi.org/10.1159/000113560

Gleich, O., Dooling, R.J., Manley, G.A., 2005. Audiogram, body mass, and basilar papilla length: correlations in birds and predictions for extinct archosaurs. Naturwissenschaften 92, 595–598. https://doi.org/10.1007/s00114-005-0050-5

Gummer, A.W., Smolders, J.W.Th., Klinke, R., 1989. Mechanics of a single-ossicle ear: I. The extra-stapedius of the pigeon. Hear. Res. 39, 1–13. https://doi.org/10.1016/0378-5955(89)90077-4

Heffner, H.E., Heffner, R.S., 2007. Evolution of mammalian hearing. J. Acoust. Soc. Am. 121, 3052–3052.
Heffner, R.S., 2004. Primate hearing from a mammalian perspective. Anat. Rec. A. Discov. Mol. Cell. Evol. Biol. 281A, 1111–1122. https://doi.org/10.1002/ar.a.20117
Heffner, H.E., Koay, G., Heffner, R.S., 2016. Budgerigars (*Melopsittacus undulatus*) do not hear infrasound: the audiogram from 8 Hz to 10 kHz. J. Comp. Physiol. A 202, 853–857. https://doi.org/10.1007/s00359-016-1125-9
Heffner, H.E., Koay, G., Hill, E.M., Heffner, R.S., 2013. Conditioned suppression/avoidance as a procedure for testing hearing in birds: The domestic pigeon (*Columba livia*). Behav. Res. Methods 45, 383–392. https://doi.org/10.3758/s13428-012-0269-y
Heffner, R., Cumming, J.F., Koay, G., Heffner, H.E., 2020. Hearing in Indian peafowl (*Pavo cristatus*): sensitivity to infrasound. J. Comp. Physiol. A. https://doi.org/10.1007/s00359-020-01446-2
Hemilä, S., Nummela, S., Reuter, T., 1995. What middle ear parameters tell about impedance matching and high frequency hearing. Hear. Res. 85, 31–44. https://doi.org/10.1016/0378-5955(95)00031-X
Hetherington, T.E., 1992. The Effects of Body Size on Functional Properties of Middle Ear Systems of Anuran Amphibians. Brain. Behav. Evol. 39, 133–142. https://doi.org/10.1159/000114111
Hill, E.M., 2017. Audiogram of the mallard duck (*Anas platyrhynchos*) from 16 Hz to 9 kHz. J. Comp. Physiol. A 203, 929–934. https://doi.org/10.1007/s00359-017-1204-6
Hill, E.M., Koay, G., Heffner, R.S., Heffner, H.E., 2014. Audiogram of the chicken (Gallus gallus domesticus) from 2 Hz to 9 kHz. J. Comp. Physiol. A 200, 863–870. https://doi.org/10.1007/s00359-014-0929-8
James, L.S., Taylor, R.C., Hunter, K.L., Ryan, M.J., 2021. Evolutionary and allometric insights into anuran auditory sensitivity and morphology. Brain. Behav. Evol. https://doi.org/10.1159/000521309
Jensen, K.K., Klokker, S., 2006. Hearing sensitivity and critical ratios of hooded crows (Corvus corone cornix). J. Acoust. Soc. Am. 119, 1269–1276. https://doi.org/10.1121/1.2159431
Kirk, E.C., Gosselin-Ildari, A.D., 2009. Cochlear labyrinth volume and hearing abilities in primates. Anat. Rec. Hoboken NJ 2007 292, 765–776. https://doi.org/10.1002/ar.20907
Klump, G.M., Kretzschmar, E., Curio, E., 1986. The hearing of an avian predator and its avian prey. Behav. Ecol. Sociobiol. 18, 317–323. https://doi.org/10.1007/BF00299662
Köppl, C., 2009. Evolution of sound localisation in land vertebrates. Curr. Biol. 19, R635–R639. https://doi.org/10.1016/j.cub.2009.05.035
Larsen, O.N., Christensen-Dalsgaard, J., Jensen, K.K., 2016. Role of intracranial cavities in avian directional hearing. Biol. Cybern. 110, 319–331. https://doi.org/10.1007/s00422-016-0688-4
Manley, G.A., 1995. The lessons of middle-ear function in non-mammals: improving columellar prostheses. J. R. Soc. Med. 88, 367–368.
Mason, M.J., 2016. Structure and function of the mammalian middle ear. II: Inferring function from structure. J. Anat. 228, 300–312. https://doi.org/10.1111/joa.12316
Mason, M.J., Farr, M.R.B., 2013. Flexibility within the middle ears of vertebrates. J. Laryngol. Otol. 127, 2–14. https://doi.org/10.1017/S0022215112002496

Maxwell, A., Hansen, K.A., Ortiz, S.T., Larsen, O.N., Siebert, U., Wahlberg, M., 2017. In-air hearing of the great cormorant (*Phalacrocorax carbo*). Biol. Open 6, 496–502. https://doi.org/10.1242/bio.023879
Muyshondt, P.G.G., Aerts, P., Dirckx, J.J.J., 2016. Acoustic input impedance of the avian inner ear measured in ostrich (*Struthio camelus*). Hear. Res. 339, 175–183. https://doi.org/10.1016/j.heares.2016.07.009
Muyshondt, P.G.G., Dirckx, J.J.J., 2019. How flexibility and eardrum cone shape affect sound conduction in single-ossicle ears: a dynamic model study of the chicken middle ear. Biomech. Model. Mechanobiol. https://doi.org/10.1007/s10237-019-01207-4
Nummela, S., 1995. Scaling of the mammalian middle ear. Hear. Res. 85, 18–30. https://doi.org/10.1016/0378-5955(95)00030-8
Nummela, S., 1997. Scaling and modeling the mammalian middle ear. Comments Theor. Biol., 4, 387–412.
Nummela, S., Sánchez-Villagra, M.R., 2006. Scaling of the marsupial middle ear and its functional significance. J. Zool. 270, 256–267. https://doi.org/10.1111/j.1469-7998.2006.00126.x
Okanoya, K., Dooling, R.J., 1987. Hearing in passerine and psittacine birds: A comparative study of absolute and masked auditory thresholds. J. Comp. Psychol. 101, 7–15. https://doi.org/10.1037/0735-7036.101.1.7
Peacock, J., Spellman, G.M., Greene, N.T., Tollin, D.J., 2020. Scaling of the avian middle ear. Hear. Res. 108017. https://doi.org/10.1016/j.heares.2020.108017
Plassmann, W., Brändle, K., 1992. A Functional Model of the Auditory System in Mammals and Its Evolutionary Implications, in: Webster, D.B., Popper, A.N., Fay, R.R. (Eds.), The Evolutionary Biology of Hearing. Springer New York, pp. 637–653.
Prum, R.O., Berv, J.S., Dornburg, A., Field, D.J., Townsend, J.P., Lemmon, E.M., Lemmon, A.R., 2015. A comprehensive phylogeny of birds (Aves) using targeted next-generation DNA sequencing. Nature 526, 569–573. https://doi.org/10.1038/nature15697
R Core Team, 2020. R: A Language and Environment for Statistical Computing. R Foundation for Statistical Computing, Vienna, Austria.
Rosowski, J., Graybeal, A., 1991. What did Morganucodon hear? Zool. J. Linn. Soc. 101, 131–168.
Rosowski, J.J., 1994. Outer and Middle Ears, in: Fay, R.R., Popper, A.N. (Eds.), Comparative Hearing: Mammals, Springer Handbook of Auditory Research. Springer New York, New York, NY, pp. 172–247. https://doi.org/10.1007/978-1-4612-2700-7_6
Saunders, J.C., Duncan, R.K., Doan, D.E., Werner, Y.L., 2000. The Middle Ear of Reptiles and Birds, in: Dooling, R.J., Fay, R.R., Popper, A.N. (Eds.), Comparative Hearing: Birds and Reptiles, Springer Handbook of Auditory Research. Springer New York, pp. 13–69.
Schwing, R., Nelson, X.J., Parsons, S., 2016. Audiogram of the kea parrot, *Nestor notabilis*. J. Acoust. Soc. Am. 140, 3739–3744. https://doi.org/10.1121/1.4967757
Strawn, S.N., Hill, E.M., 2020. Japanese quail (*Coturnix japonica*) audiogram from 16 Hz to 8 kHz. 206, 665–670 J. Comp. Physiol. A. https://doi.org/10.1007/s00359-020-01428-4
Trainer, J.E., 1946. Auditory acuity of certain birds (PhD Thesis). Graduate School of Cornell University.
Van Dijk, T., 1972. A comparative study of hearing in owls of the family Strigidae. Neth. J. Zool. 23, 131–167.

Walsh, S.A., Barrett, P.M., Milner, A.C., Manley, G., Witmer, L.M., 2009. Inner ear anatomy is a proxy for deducing auditory capability and behaviour in reptiles and birds. Proc. R. Soc. Lond. B Biol. Sci. 276, 1355–1360. https://doi.org/10.1098/rspb.2008.1390

Werner, Y.L., Igić, P.G., 2002. The middle ear of gekkonoid lizards: interspecific variation of structure in relation to body size and to auditory sensitivity. Hear. Res. 167, 33–45. https://doi.org/10.1016/S0378-5955(02)00331-3

Werner, Y.L., Igić, P.G., Seifan, M., Saunders, J.C., 2002. Effects of age and size in the ears of gekkonomorph lizards: middle-ear sensitivity. J. Exp. Biol. 205, 3215–3223.

Werner, Y.L., Montgomery, L.G., Seifan, M., Saunders, J.C., 2008. Effects of age and size in the ears of gekkotan lizards: auditory sensitivity, its determinants, and new insights into tetrapod middle-ear function. Pflüg. Arch. - Eur. J. Physiol. 456, 951. https://doi.org/10.1007/s00424-008-0462-0

Wright, T.F., Cortopassi, K.A., Bradbury, J.W., Dooling, R.J., 2003. Hearing and vocalizations in the orange-fronted conure (*Aratinga canicularis*). J. Comp. Psychol. Wash. DC 1983 117, 87–95. https://doi.org/10.1037/0735-7036.117.1.87

Zdilla, M.J., Skrzat, J., Kozerska, M., Leszczyński, B., Tarasiuk, J., Wroński, S., 2018. Oval window size and shape: A micro-CT anatomical study with considerations for stapes surgery. Otol. Neurotol. Off. Publ. Am. Otol. Soc. Am. Neurotol. Soc. Eur. Acad. Otol. Neurotol. 39, 558–564. https://doi.org/10.1097/MAO.0000000000001787

Zeyl, J.N., Snelling, E.P., Connan, M., Basille, M., Clay, T.A., Joo, R., Patrick, S.C., Phillips, R.A., Pistorius, P.A., Ryan, P.G., Snyman, A., Clusella-Trullas, S., 2022. Aquatic birds have middle ears adapted to amphibious lifestyles. Sci. Rep. 12, 5251. https://doi.org/10.1038/s41598-022-09090-3